ISSN 0036-0236, Russian Journal of Inorganic Chemistry, 2016, Vol. 61, No. 2, pp. 161–167. © Pleiades Publishing, Ltd., 2016.
Original Russian Text © N.N. Bushuev, D.S. Zinin, 2016, published in Zhurnal Neorganicheskoi Khimii, 2016, Vol. 61, No. 2, pp. 173–179.

SYNTHESIS AND PROPERTIES OF INORGANIC COMPOUNDS

Thermal Decomposition Features of Calcium and Rare-Earth Oxalates

N. N. Bushuev and D. S. Zinin

Mendeleev University of Chemical Technology, Moscow, Russia

e-mail: nbushuev@muctr.ru

Received March 13, 2015

Abstract—Thermal decomposition of $Ln_2(C_2O_4)_3 \cdot 9H_2O$ concentrate (Ln = La, Ce, Pr, Nd) in the presence of $CaC_2O_4 \cdot H_2O$ was studied by X-ray diffraction, thermogravimetry, and chemical analysis. Annealing at temperatures above 374°C in the absence of calcium oxalate gives rise to the solid solution of CeO_2-based rare-earth oxides. Calcite $CaCO_3$ is formed in the presence of calcium oxalate at annealing temperatures above 442°C, which impedes the formation of lanthanide oxide solid solution and favors crystallization of oxides as individual La_2O_3, CeO_2, Pr_6O_{11}, and Nd_2O_3 phases. An increase in temperature above 736°C is accompanied by decomposition of calcium carbonate to give rise to an individual CaO phase and an individual phase of CeO_2-based lanthanide oxide solid solution.

DOI: 10.1134/S0036023616020030

The $2Ca^{2+} = Na^+ + Ln^{3+}$ isomorphic substitution boundaries in binary systems $CaSO_4 \cdot 0.5H_2O$–$NaLn(SO_4)_2 \cdot H_2O$ and $CaSO_4$–$NaLn(SO_4)_2$, where Ln = La, Ce, or Nd, were studied in [1–3]; $Ca^{2+} = Sr^{2+}$ isomorphic substitutions boundaries in the systems $CaSO_4 \cdot 0.5H_2O$–$SrSO_4$ and $CaSO_4$–$SrSO_4$ were studied in [4, 5]. Based on these studies, an assumption was made that $CaSO_4 \cdot 0.5H_2O$ can potentially be used for cocrystallizing lanthanides and strontium in the calcium sulfate matrix, yielding a solid solution based on the $CaSO_4 \cdot 0.5H_2O$ structure upon Kola apatite decomposition using sulfuric acid in the production of phosphoric acid by the wet process. The resulting calcium sulfate precipitates contained up to 5 wt % of lanthanides. Earlier attempts to extract rare-earth elements by thermal treatment of the sulfate precipitate have been unsuccessful [6].

The best results were shown by oxalate conversion of the sulfate precipitate, giving rise to $CaC_2O_4 \cdot H_2O$ and $Ln_2(C_2O_4)_3 \cdot 9H_2O$ oxalate precipitates [7, 8]. Production of pure rare-earth concentrates is a challenging task, which is typically fulfilled using ion-exchange resins and expensive equipment [9]. Hence, searching for simpler methods for separating lanthanides and calcium is a relevant research problem.

Thermal decomposition of calcium and rare-earth oxalates has recently been used to produce various materials. Several groups of rare-earth-containing oxide materials are currently differentiated: solid solutions of rare-earth oxides [10, 11], individual rare-earth oxides [12], and solid solutions of alkaline earth metals and rare-earth [13–16]. A noticeable preference is given to the production of these materials using intermediate oxalate compounds, since their precipitation and subsequent thermal decomposition gives rise to homogeneous oxide phases at relatively low temperatures, thus making it possible to retain the catalytic activity as well as the thermal and mechanical stability of the resulting compounds [17–20].

It should be mentioned that rare-earth-containing calcium oxalate is an intermediate product in the large-scale extraction of rare earths from some natural minerals. This means that this mixture can be used to produce the aforelisted oxide materials via thermal treatment.

This study focuses on the features of thermal decomposition of calcium oxalate containing rare-earth oxalate impurities and the relatively pure oxalate concentrate of rare earths. Comparing these thermochemical processes makes it possible to ascertain what effect REE impurities have on the phase composition of the decomposition products and the phase transition temperature. While sparse data on using individual rare-earth-based compounds (e.g., those based on La, Sm, or Gd) to catalyze thermal decomposition of $CaC_2O_4 \cdot H_2O$ are available in literature [21, 22], this study is the first one to address thermal decomposition of mixtures of calcium and rare-earth oxalates produced by oxalate conversion of sulfate precipitates.

EXPERIMENTAL

Chemical analysis of the samples was carried out at the Analytical Certification Testing Center (All-Russian Research Institute of Mineral Resources, Mos-

Table 1. Chemical analysis (wt %) of rare-earth -containing samples under study

Element	Oxalate, precipitate	Oxalate, concentrate [10]	Analysis method	Element	Oxalate, precipitate	Oxalate, concentrate [10]	Analysis method
F	0.13	<0.02	IM	Nd	1.12	9.9	MS
Na	0.03	<0.01	AE	Sm	0.15	1.8	MS
Al	0.042	0.029	AE	Eu	0.041	0.47	MS
Si	0.040	0.16	PhM	Gd	0.12	1.3	MS
P	0.037	<0.001	PhM	Tb	0.013	0.13	MS
S	0.015	<0.002	GrM	Dy	0.040	0.43	MS
Ca	20.6	0.31	GrM	Ho	0.0045	0.05	MS
Sc	0.0001	<0.002	MS	Er	0.0077	0.074	MS
Ti	<0.0004	<0.0002	MS, AE	Tm	0.00043	0.004	MS
Fe	<0.006	<0.003	MS, AE	Yb	0.00131	0.015	MS
As	0.0012	<0.0007	MS	Lu	0.00015	0.0013	MS
Sr	0.35	0.0038	MS, AE	Hg	<0.00002	<0.00006	MS
Y	0.11	0.88	MS	Pb	0.0013	0.00092	MS, AE
Cd	<0.00002	<0.0001	MS, AE	Th	0.00093	0.0039	MS
La	0.94	5.3	MS	U	<0.00002	<0.00005	MS
Ce	2.41	17	MS	$\sum Ln + Y$	5.28	39.97	
Pr	0.32	2.6	MS	$\sum Ln_2O_3 + Y_2O_3$	6.18	46.78	

cow, Russia) using the following methods: inductively coupled plasma mass spectrometry (MS) on an Elan-6100 system, inductively coupled plasma atomic emission spectroscopy (AE) on an Optima-4300 DV instrument, gravimetric analysis (GrM), photometric analysis (PhM), and ionometric analysis (IM). Thermogravimetric analysis (TGA) and differential scanning calorimetry (DSC) of the samples was carried out on a Netzsch STA 409 PC simultaneous thermal analyzer in the TG–DSC mode in a dynamic air flow (30 mL/min) under heating to 1000 or 1400°C at a constant rate of 1°C/min. An oxalate sample weighing ~8.0 or 10 mg was placed in corundum crucibles and heated. The detected endo- and exothermic extrema on the DSC curve were attributed to phase transformations. After the sample was annealed for 1 h at the corresponding temperatures, their phase compositions was determined.

X-ray diffraction analysis (XRD) of the samples was carried out with a G670 monochromator camera ($CuK_{\alpha 1}$ radiation).

A calcium oxalate sample with REE oxalates as an impurity was prepared by oxalate conversion of the calcium sulfate precipitate extracted from technical grade phosphoric acid containing rare earths. The oxalate precipitate was dissolved in nitric acid (chemically pure grade) to obtain a rare earth oxalate concentrate sample [7, 8, 10]. Table 1 lists the chemical compositions of the compounds under study.

RESULTS AND DISCUSSION

X-ray powder diffraction and chemical analysis of the rare-earth-containing calcium oxalate precipitate showed the following phases: 74–78 wt % of $CaC_2O_4 \cdot H_2O$, 7–9 wt % of $CaC_2O_4 \cdot 2.25H_2O$, and 13–16 wt % of the X-ray amorphous $Ln_2(C_2O_4)_3 \cdot nH_2O$ phase. It should be mentioned that the XRD pattern features diffraction lines of the aforelisted calcium oxalates only (ICDD 20-231 and 20-233). The absence of the characteristic lines of $Ln_2(C_2O_4)_3 \cdot nH_2O$ in the XRD pattern is most likely associated with adsorption of the highly disperse X-ray amorphous phase of rare-earth oxalates on the surface of calcium oxalate hydrate crystals [7–10, 21, 22].

The phase and chemical compositions of the pure oxalate concentrate of $Ln_2(C_2O_4)_3 \cdot 9H_2O$ was confirmed by X-ray diffraction analysis, mass spectroscopy, and TGA. The impurity content in the sample of oxalate concentrate of REEs under study was less than 1 wt % [10].

The resulting oxalate samples mostly contain cerium-subgroup elements (La–Sm), which are up to 95 rel. % of the total content of REEs. The content of lanthanides with even atomic numbers (Ce, Nd, Sm, Gd, and Dy) is higher than that of lanthanides with odd atomic numbers (La, Pr, Eu, and Tb), which agrees with the Oddo–Harkins rule for a natural mixture of rare earths (Table 1).

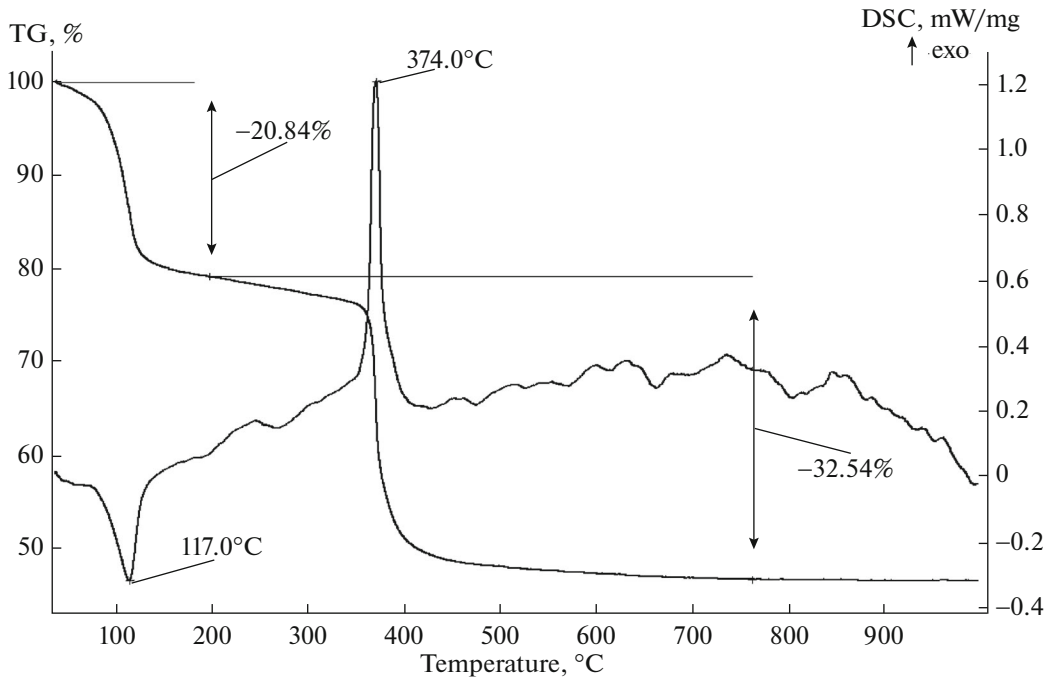

Fig. 1. Thermal decomposition of pure rare-earth oxalate concentrate.

The main stages of thermal decomposition of calcium and rare-earth oxalate crystal hydrates in air are as follows:

1) dehydration of oxalates:

$$CaC_2O_4 \cdot mH_2O = CaC_2O_4 + mH_2O, \quad (1a)$$

$$Ln_2(C_2O_4)_3 \cdot nH_2O = Ln_2(C_2O_4)_3 + nH_2O; \quad (1b)$$

2) oxidation of anhydrous oxalates in air:

$$CaC_2O_4 + 0.5O_2 = CaCO_3 + CO_2, \quad (2a)$$

$$Ln_2(C_2O_4)_3 + xO_2 = 2LnO_x + 6CO_2; \quad (2b)$$

3) decomposition of carbonates:

$$CaCO_3 = CaO + CO_2. \quad (3)$$

The dehydration of calcium and rare-earth oxalates (1a) and (1b), as well as the reaction of decomposition of calcium carbonate (3), are accompanied with endoterms on the DSC curve. As opposed to these processes, the oxidation reactions of calcium and rare-earth oxalates (2a) and (2b) in air are accompanied with exotherms.

Figures 1 and 2 show the results of simultaneous TG–DSC studies of the thermal decomposition of samples of a rare-earth concentrate and calcium oxalate with rare-earth oxalate impurity in air.

The decomposition mechanism for a calcium oxalate sample with a rare-earth oxalate impurity is similar to that for pure $CaC_2O_4 \cdot H_2O$ [21, 22]. Nevertheless, the emergence of a small exotherm at 385°C indicates that the sample contains rare-earth oxalates. In order to determine the thermal co-decomposition features of calcium and rare-earth oxalates, we thermogravimetrically studied a sample of pure rare-earth oxalate concentrate containing no calcium.

For the pure rare-earth oxalate concentrate, dehydration ends at 117°C. The weight loss by a 20.48 wt % sample corresponds to removal of nine water molecules.

X-ray diffraction analysis of the sample of rare-earth oxalate concentrate annealed at 250°C in air showed an X-ray amorphous structure. The resulting mixture of anhydrous rare-earth oxalates was stable over a broad temperature range (117–374°C).

The calcium oxalate sample with rare-earth an oxalate impurity was annealed in air at 125°C. XRD showed that the sample retained the $CaC_2O_4 \cdot H_2O$ structure (ICDD 20-231), while the XRD pattern contained no lines corresponding to $CaC_2O_4 \cdot 2.25H_2O$ (ICDD 20-0233).

Complete dehydration of the calcium oxalate sample containing rare-earth oxalate impurities (Fig. 2) takes place at a higher temperature (190°C) compared to the dehydration temperature of $Ln_2(C_2O_4)_3 \cdot 9H_2O$ (117°C) (Fig. 1). The first value corresponds to the dehydration temperature of pure $CaC_2O_4 \cdot H_2O$ reported in [16]. The significant weight loss (13.48 wt %) by the calcium oxalate sample containing REE oxalates was caused by complete dehydration of $CaC_2O_4 \cdot H_2O$, $CaC_2O_4 \cdot 2.25H_2O$, and $Ln_2(C_2O_4)_3 \cdot 9H_2O$ (76, 8, and 16 wt %, respectively).

It was found that oxidation of pure anhydrous rare-earth oxalate concentrate in air takes place at 374°C

Table 2. Results of X-ray analysis of a calcium carbonate sample containing rare-earth oxides

Sample under study		$CaCO_3$ ICDD 05-0586		La_2O_3 ICDD 22-0369		Nd_2O_3 ICDD 21-0579		Pr_6O_{11} ICDD 06-0329		CeO_2 ICDD 34-394	
d, Å	*I*, %	*d*, Å	*I*, %	*d*, Å	*I*, %	*d*, Å	*I*, %	*d*, Å	*I*, %	*d*, Å	*I*, %
3.854	9	3.860	12								
3.244	3			3.267	100						
3.202	8					3.198	100				
3.162	12							3.154	100		
3.123	4									3.123	100
3.040	100	3.035	100								
2.850	1	2.845	3								
2.824	2			2.830	35						
2.768	2					2.770	60				
2.735	3							2.734	35		
2.704	1									2.706	30
2.492	13	2.495	14								
2.285	17	2.285	18								
2.093	16	2.095	18								
1.9949	2			2.001	40						
1.9557	4					1.9574	70				
1.9317	11	1.9270	5					1.9336	50		
1.9188	16	1.9130	17							1.9135	52
1.8782	18	1.8750	17								
1.7001	1			1.7006	25						
1.6651	3			1.6676	10	1.6686	65				
1.6498	3							1.6486	40		
1.6263	3	1.6260	4					1.6327	6	1.6318	42
1.6033	7	1.6040	8								
1.5240	5	1.5250	5								
1.5139	2	1.5180	4								
1.4741	2	1.4730	2								
1.4395	5	1.4400	5								
1.4282	2	1.4220	3								
1.3894	1					1.3839	10				
1.3712	2							1.3667	8		
1.3581	1	1.3560	1							1.3531	8
1.3415	1	1.3390	2								
1.2986	2	1.2970	2	1.2969	10						
1.2785	1	1.2840	1	1.2650	10	1.2699	18				
1.2472	2	1.2470	1			1.2380	10	1.2546	14		
1.2390	2	1.2350	2					1.2231	10	1.2415	14
1.1823	2	1.1795	3							1.2101	8
1.1536	3	1.1538	3								

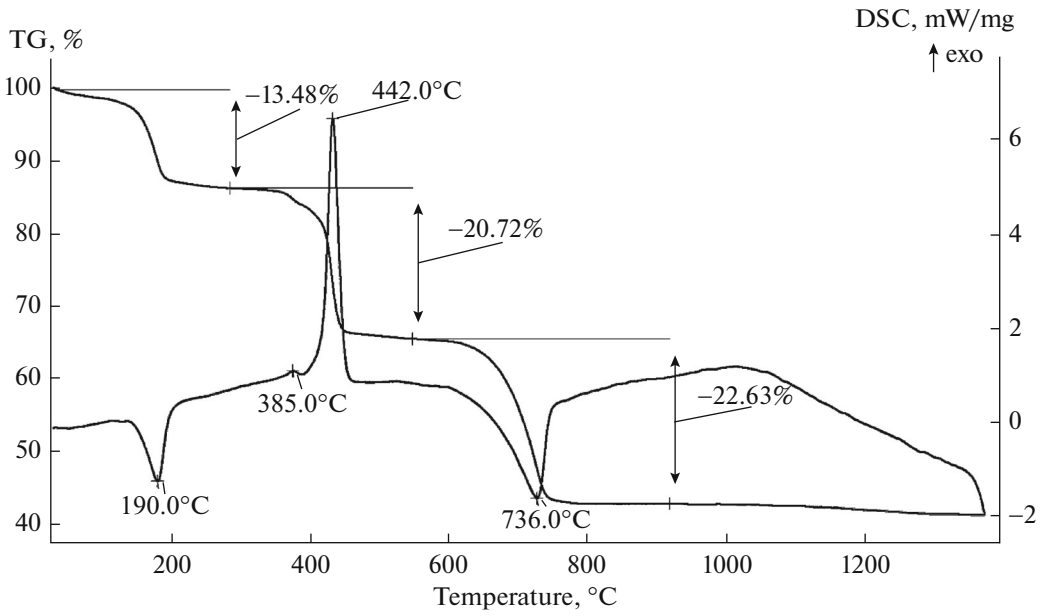

Fig. 2. Thermal decomposition of calcium oxalate-containing rare-earth oxalates.

(Fig. 1), giving rise to the rare-earth oxide solid solution with the unit cell parameters as determined in [10]: space group *Fm*3*m*, $a = 5.487(15)$ Å, $Z = 4$, $V = 165.2(8)$ Å^3. The weight of the resulting rare-earth oxide concentrate was 47 rel. % of the weight of the initial oxalate concentrate.

Oxidation of the mixture of anhydrous rare-earth oxalates to oxides in the presence of anhydrous calcium oxalates ends at almost the same temperature (385°C) and is accompanied by a small exotherm on the DSC curve (Fig. 2). The next pronounced exotherm (442°C) corresponds to the oxidation of anhydrous calcium oxalate to calcium carbonate. The total weight loss by the sample at this stage is 34.5 wt %.

Oxidation of anhydrous calcium oxalate to carbonate in air in the presence of rare-earth oxides takes place at 442°C; this temperature is appreciably close to the temperature at which pure calcium oxalate decomposes (460°C) [21, 22].

The XRD pattern of the sample of calcium oxalate containing rare-earth oxalates annealed at 550°C in air (Table 2) features diffraction lines belonging to $CaCO_3$ (calcite, space group *R*3*c*) and oxides of cerium-subgroup rare-earth: La_2O_3, Nd_2O_3 (space group *Ia*3) and CeO_2, Pr_6O_{11} (space group *Fm*3*m*).

Calcium carbonate containing rare-earth oxide impurities undergoes thermal decomposition at 736°C, giving rise to the corresponding oxide. The presence of phases of rare-earth oxides makes the decomposition temperature of $CaCO_3$ decrease from 875 to 736°C.

Table 3 lists the results of XRD of the calcium oxalate sample containing rare-earth oxalates annealed at 1000°C. The sample consists of two phases: 80 wt % CaO and 20 wt % solid solution of rare-earth oxides based on the CeO_2 structure, which crystallize in a cubic lattice (space group *Fm*3*m*). The weight loss for the initial sample is as high as 56.83 wt %, which agrees with the theoretical calculations.

It is important to mention that the XRD pattern of this sample does not show any shift of the lines belonging to the CaO phase (ICDD 48-1467); hence, one can assume that the thermodynamically stable form of the CaO-based solid solution is not formed at 1000°C. Thermal co-decomposition of calcium and rare-earth oxalates ends with the formation of an individual CaO phase and the phase of rare-earth oxide solid solution, which agrees with the previously published findings [21, 22]. Based on the XRD data of the two-phase sample containing calcium oxide and the solid solution of rare-earth oxides listed in Table 3, we determined the unit cell parameters of the phase of solid solution of lanthanide oxides: space group. *Fm*3*m*, $a = 5.507(15)$ Å, $Z = 4$, and $V = 167.0$ Å^3. These parameters are similar to those of pure rare-earth oxide concentrate: $a = 5.487(15)$ Å, $Z = 4$, and $V = 165.2(8)$ Å^3, determined in [10], thus proving an insignificant difference between the lanthanide ratios in the aforelisted samples of rare-earth oxide solid solutions. This difference results from the difference in lanthanide ratio in their precursors, rare-earth oxalates (Table 1). Thus, the Nd : ∑Ln + Y ratio in the oxalate precipitate under study is 1.12 : 5.28 = 0.21. In the single-phase oxalate concentrate obtained from nitrate solutions in [10], this ratio is 9.9 : 39.97 = 0.25. The increased ratio of smaller rare-earth ions for the La–Ce–Pr–Nd series is accompanied by a decrease in unit cell param-

Table 3. Results of X-ray diffraction analysis of a sample containing calcium oxide and rare-earth oxide solid solution

Sample under study		Rare-earth oxide solid solution [10]			CaO, ICDD 48-1467		
d, Å	*I*, %	*d*, Å	*I*, %	*h k l*	*d*, Å	*I*, %	*h k l*
3.177	100	3.160	100	1 1 1			
2.776	38				2.778	40	1 1 1
2.752	28	2.756	30	2 0 0			
2.405	89				2.405	100	2 0 0
1.9470	58	1.9394	38	2 2 0			
1.7011	61				1.7008	51	2 2 0
1.6603	35	1.6535	28	3 1 1			
1.5899	6	1.5767	5	2 2 2			
1.4511	17				1.4504	17	3 1 1
1.3894	16				1.3887	14	2 2 2
1.3769	6	1.3724	5	4 0 0			
1.2635	11	1.2612	5	3 3 1			
1.2315	6	1.2259	9	4 2 0			
1.2034	9				1.2026	6	4 0 0

eters of the solid solution, which is not related to the effect of CaO.

Depending on the products formed during decomposition of oxalates in air, thermal transformations of oxalate crystal hydrates are subdivided into three stages: dehydration, oxidation, and decarboxylation. Formation of the final oxide phase is associated with the features of formation and growth of crystals of intermediate products and their interaction during thermal treatment.

Dehydration of the mixture of crystal hydrates of calcium and rare-earth oxalates is a simultaneous process at 190°C. It should be mentioned that the presence of a significant amount of cerium(III) oxalate hydrate in the sample also favors one-stage dehydration of the entire mixture of calcium and rare-earth oxalates, which agrees with previously published data [10, 17–20].

The results of the TGA/DSC/XRD studies confirmed that the oxidation of a mixture of anhydrous rare-earth and calcium oxalates includes two sequential stages (Fig. 2), resulting in the formation of rare-earth oxide phases at 385°C and the calcium carbonate phase at 442°C. Hence, the mixture components, calcium and rare-earth oxalates, retain their individuality in the dehydrated mixture.

During annealing in air, decomposition of rare-earth oxalates to oxides (except for cerium oxalates) is accompanied by the formation of intermediate phases of rare-earth carbonates and oxycarbonates [17–20]. In our study, the samples contained large amounts of cerium oxalate; hence, thermal decomposition of an isomorphic mixture of rare-earth oxalates in air included one stage and gave rise to a mixture of rare-earth oxides.

It has been found that annealing of a calcium oxalate sample containing rare-earth oxalates at temperatures above 442°C gives rise to calcite $CaCO_3$, which impedes the formation of a lanthanide oxide solid solution and promotes their crystallization as individual phases La_2O_3, CeO_2, Pr_6O_{11}, and Nd_2O_3. No other $CaCO_3$ crystal polymorphs were found to be formed in this study.

Calcium carbonate decomposes at temperatures above 736°C, giving rise to individual phases of CaO and lanthanide oxidesolid solution. The presence of rare-earth oxide phases in the mixture reduces the decomposition temperature of $CaCO_3$ from 875 to 736°C, which agrees with earlier findings [21, 22].

The thermal treatment of calcium oxalate containing rare-earth oxalates at 450°C can be one of the steps of extraction and concentration of rare earths as individual oxides after the main $CaCO_3$ phase was removed. Preliminary removal of calcium compounds from the rare-earth oxalate concentrate prior to thermal treatment may favor the formation of rare-earth oxide solid solution . Hence, heat treatment of an oxalate precipitate containing Ca and REEs can be a promising method for extracting and concentrating rare earths.

REFERENCES

1. N. N. Bushuev, A. Ya. Tavrovskaya, S. N. Babaev, and A. N. Egorova, Zh. Neorg. Khim. **34**, 179 (1989).
2. N. N. Bushuev, O. N. Efremov, and A. Ya. Tavrovskaya, Zh. Neorg. Khim. **33**, 743 (1988).

3. N. N. Bushuev, A. Ya. Tavrovskaya, and P. M. Zaitsev, Zh. Neorg. Khim. **33**, 2420 (1988).
4. N. N. Bushuev and A. G. Nabiev, Zh. Neorg. Khim. **33**, 2962 (1988).
5. N. N. Bushuev, N. S. Nikonova, and N. V. Mishenina, Zh. Neorg. Khim. **33**, 531 (1988).
6. N. N. Bushuev and D. S. Zinin, Khim. Prom. Segodnya, No. **5**, 16 (2014).
7. N. N. Bushuev and B. V. Levin, Khim. Tekhnol., No. 1, 52 (2014).
8. N. N. Bushuev, D. S. Zinin, and B. V. Levin, Khim. Tekhnol., No. 9, 549 (2014).
9. J. R. Webster and M. S. Gilstrap, Chem. Geol. **85**, 287 (1990).
10. D. S. Zinin and N. N. Bushuev, Russ. J. Appl. Chem. **87**, 1611 (2014).
11. O. S. Ivanova, E. A. Dolgopolova, A. E. Baranchikov, et al., Russ. J. Inorg. Chem. **56**, 1688 (2011).
12. V. N. Lebedev and A. V. Rudenko, Russ. J. Appl. Chem. **75**, 1357 (2002).
13. N. M. Ghoneim, M. A. Mandour, and M. A. Serry, Ceram. Int. **15**, 357 (1989).
14. N. M. Ghoneim, M. A. Mandour, and M. A. Serry, Ceram. Int. **16**, 215 (1990).
15. M. Dudek and K. Ziewiec, Adv. Mater. Sci. **6**, 4 (2006).
16. B. Savova, D. Filkova, D. Crisan, et al., Appl. Catal., A **359**, 47 (2009).
17. B. A. A. Balboul, A. M. El-Roudi, E. Samir, and A. G. Othman, Thermochim. Acta, No. 387, 109 (2002).
18. L. De Almeida, S. Grandjean, N. Vigier, and F. Patisson, Eur. J. Inorg. Chem. **2012**, 4986 (2012).
19. S. El-Houte and AliM. EI-Sayed, J. Therm. Anal. **37**, 907 (1991).
20. V. A. Matyukha and S. V. Matyukha, Rare-Earth and Actinid Oxalates (Energoatomizdat, Moscow, 2004) [in Russian].
21. S. Bose, K. K. Sahu, and D. Bhatta, Thermochim. Acta, No. 268, 175 (1995).
22. U. Patnaik and J. Muralidhar, Thermochim. Acta, No. 274, 261 (1996).

Translated by D. Terpilovskaya